Inorg. Chem. **2007**, *46*, 541–551

^{63}Cu NMR Spectroscopy of Copper(I) Complexes with Various Tridentate Ligands: CO as a Useful ^{63}Cu NMR Probe for Sharpening ^{63}Cu NMR Signals and Analyzing the Electronic Donor Effect of a Ligand

Masato Kujime, Takuya Kurahashi, Masaaki Tomura, and Hiroshi Fujii*

Institute for Molecular Science and Okazaki Institute for Integrative Bioscience, National Institutes of Natural Sciences, Myodaiji, Okazaki 444-8787, Japan

Received May 2, 2006

^{63}Cu NMR spectroscopic studies of copper(I) complexes with various N-donor tridentate ligands are reported. As has been previously reported for most copper(I) complexes, ^{63}Cu NMR signals, when acetonitrile is coordinated to copper(I) complexes of these tridentate ligands, are broad or undetectable. However, when CO is bound to tridentate copper(I) complexes, the ^{63}Cu NMR signals become much sharper and show a large downfield shift compared to those for the corresponding acetonitrile complexes. Temperature dependence of ^{63}Cu NMR signals for these copper(I) complexes show that a quadrupole relaxation process is much more significant to their ^{63}Cu NMR line widths than a ligand exchange process. Therefore, an electronic effect of the copper bound CO makes the ^{63}Cu NMR signal sharp and easily detected. The large downfield shift for the copper(I) carbonyl complex can be explained by a paramagnetic shielding effect induced by the copper bound CO, which amplifies small structural and electronic changes that occur around the copper ion to be easily detected in their ^{63}Cu NMR shifts. This is evidenced by the correlation between the ^{63}Cu NMR shifts for the copper(I) carbonyl complexes and their ν(C≡O) values. Furthermore, the ^{63}Cu NMR shifts for copper(I) carbonyl complexes with imino-type tridentate ligands show a different correlation line with those for amino-type tridentate ligands. On the other hand, ^{13}C NMR shifts for the copper bound ^{13}CO for these copper(I) carbonyl complexes do not correlate with the ν(C≡O) values. The X-ray crystal structures of these copper(I) carbonyl complexes do not show any evidence of a significant structural change around the Cu–CO moiety. The findings herein indicate that CO complexation makes ^{63}Cu NMR spectroscopy much more useful for Cu(I) chemistry.

Introduction

Copper complexes are known to play important roles in the active site of many copper proteins in vivo as well as in homogeneous and heterogeneous catalysis for organic chemical reactions.[1−13] For the past decades, the structures, electronic states, and reactivity of copper complexes have been widely investigated with various spectroscopic methods. UV−visible absorption, resonance Raman, and electron paramagnetic resonance spectroscopy are powerful tools for studying the structures and electronic states of copper(II) complexes because of their characteristic absorptions resulting from d−d transitions, ligand−metal charge transfers, and an unpaired electron in the copper(II) ion.[3−9] On the other hand, these spectroscopic methods have not been applied extensively to studies of copper(I) complexes because of the

* To whom correspondence should be addressed. E-mail: hiro@ims.ac.jp. Tel.: +81-564-59-5578. FAX: +81-564-59-5600.

(1) *Handbook of Metalloproteins*; Messerschmit, A., Huber, R., Poulas, T., Wieghardt, K., Eds.; John Wiley & Sons: Chichester, U.K., 2001.
(2) *Handbook on Metalloproteins*; Bertini, I., Sigel, A., Sigel, H., Eds.; Marcel Dekker: New York, 2001.
(3) Solomon, E. I.; Chen, P.; Metz, M.; Lee, S.-K.; Palmer, A. E. *Angew. Chem., Int. Ed.* **2001**, *40*, 4570−4590.
(4) Solomon, E. I.; Szilagyi, R. K.; Geroge, S. D.; Basumallick, L. *Chem. Rev.* **2004**, *104*, 419−458.
(5) Rorabacher, D. B. *Chem. Rev.* **2004**, *104*, 651−697.
(6) Henkel, G.; Kreb, B. *Chem. Rev.* **2004**, *104*, 801−824.
(7) Mirica, L. M.; Ottenwaelder, X.; Stack, T. D. P. *Chem. Rev.* **2004**, *104*, 1013−1045.
(8) Lewis, E. A.; Tolman, W. B. *Chem. Rev.* **2004**, *104*, 1047−1076.
(9) Kim, E.; Chufán, E. E.; Kamaraj, K.; Karlin, K. D. *Chem. Rev.* **2004**, *104*, 1077−1133.
(10) Nakamura, E.; Mori, S. *Angew. Chem., Int. Ed.* **2000**, *39*, 3750−3771.
(11) Thomas, A. W.; Ley, S. V. *Angew. Chem., Int. Ed.* **2003**, *42*, 5400−5449.
(12) Beletskaya, I. P.; Cheprakov, A. V. *Coord. Chem. Rev.* **2004**, *248*, 2337−2364.
(13) Pintauer, T.; Matyjaszewski, K. *Coord. Chem. Rev.* **2005**, *249*, 1155−1184.

10.1021/ic060745r CCC: $37.00
Published on Web 12/23/2006

featureless spectroscopic properties resulting from the closed shell d^{10} electron configuration of copper(I) ions.

For diamagnetic copper(I) complexes, ^{63}Cu NMR spectroscopy would appear to have the greatest potential for characterizing their structures and electronic states. ^{63}Cu NMR spectroscopy has been used in studies of copper(I) complexes both in solution and in the solid state.[14−32] For example, bimolecular rate constants for the electron-exchange processes, equilibrium constants for ligand substitution reactions, and π acceptabilities of copper bound ligands have been determined by ^{63}Cu NMR spectroscopy in solution.[16] However, the application of ^{63}Cu NMR spectroscopy has been limited to copper(I) complexes with a rigorous tetrahedral, T_d, symmetry around the copper(I) ion. This is due to fast quadrupole relaxation of the ^{63}Cu ($I = 3/2$) nucleus, which lacks rigorous T_d symmetry. As a result, only the ^{63}Cu NMR signals of copper complexes with a T_d symmetry, such as CuL_4-type complexes, are observable, and ^{63}Cu NMR signals of many copper(I) complexes with reduced symmetry, such as CuL_3L'- and $CuL_2L'_2$-type complexes, are extremely broad and frequently not even detectable.

The ^{63}Cu NMR spectrum of a copper(I) complex lacking rigorous T_d symmetry was first reported for a copper(I) carbonyl complex with a Cu_4O_4 cubane core in which each copper(I) ion binds to three *tert*-butoxides and CO with a trigonally distorted tetrahedral geometry.[22] The broad ^{63}Cu NMR signal observed at 49 ppm at 25 °C was split into a doublet ($J(^{63}Cu-^{13}C) = 800$ Hz) at 60 °C. We also successfully detected very sharp ^{63}Cu NMR signals for copper(I) carbonyl complexes with various hydrotris(1-pyrazolyl)borate (TPB) ligands even at room temperature, in spite of their C_3 symmetry around copper(I) ions.[30] In addition, the ^{63}Cu NMR chemical shifts of these complexes correlated with the ν(C≡O) values of the copper bound CO. These findings suggest that, for other copper(I) complexes, the copper bound CO may facilitate the detection of ^{63}Cu NMR signals by sharpening the signals and that CO has considerable potential as a probe in ^{63}Cu NMR spectroscopic studies intending to characterize the nature of the environment around copper ions in copper complexes.

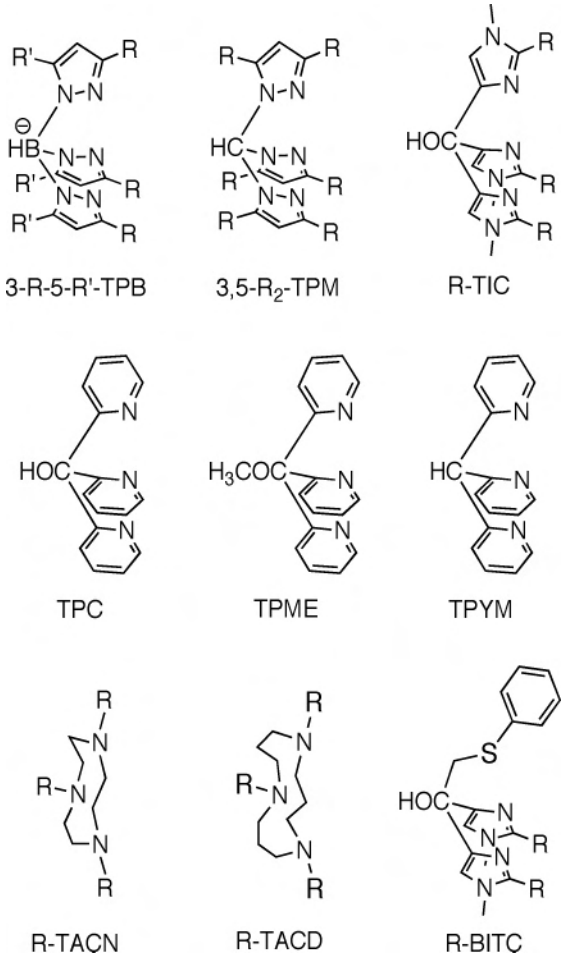

Figure 1. Structures of the N-donor tridentate ligands used in this study.

In this study, to examine the applicability of copper bound CO as a ^{63}Cu NMR probe, we obtained ^{63}Cu NMR spectra of copper(I) complexes with various N-donor tridentate ligands, in which the ligands bind to copper ions in a κ^3 manner (Figure 1). ^{63}Cu NMR signals, when CO is bound to most of the copper(I) complexes prepared in this study, become sharper and show a large downfield shift compared to those for the corresponding acetonitrile complexes. The large downfield shift in the ^{63}Cu NMR signal for the copper(I) carbonyl complexes is interpreted by a paramagnetic shielding term induced by the copper bound CO, which amplifies small structural and electronic changes that occur around the copper ion to be easily detected in their ^{63}Cu NMR shifts. On the other hand, the ^{13}C NMR shifts of the copper bound ^{13}CO of these copper(I) carbonyl complexes are nearly constant. The findings herein indicate that CO complexation makes ^{63}Cu NMR spectroscopy much more useful for Cu(I) chemistry.

(14) Ramsey, N. F. *Phys. Rev.* **1950**, *78*, 699−703.
(15) Mann, B. E. *Specialist Periodical Reports*: *Spectroscopic Properties of Inorganic and Organometallic Compounds*; Royal Society of Chemistry: London, 1990; Vol. 23, pp 1−170.
(16) Malito, J. *Annu. Rep. NMR Spectrosc.* **1999**, *38*, 265−287.
(17) Yamamoto, T.; Haraguchi, H.; Fujiwara, S. *J. Phys. Chem.* **1970**, *74*, 4369−4373.
(18) Lutz, O.; Oehler, H.; Kroneck, P. *Z. Naturforsch.* **1978**, *33A*, 1021−1024.
(19) Kroneck, P.; Lutz, O.; Nolle, A.; Oehler. H. *Z. Naturforsch*. **1980**, *35A*, 221−225.
(20) Marker, A.; Gunter, M. J. *J. Magn. Reson.* **1982**, *47*, 118−132.
(21) Kroneck, P.; Kodweiβ, J.; Lutz, O.; Nolle, A.; Zepf, D. *Z. Naturforsch.* **1982**, *37A*, 186−190.
(22) Geerts, R. L.; Huffman, J. C.; Folting, K.; Lemmen, T. H.; Caulton, K. G. *J. Am. Chem. Soc.* **1983**, *105*, 3503−3506.
(23) Kitagawa, S.; Munakata, M. *Inorg. Chem.* **1984**, *23*, 4388−4390.
(24) Nakatsuji, H.; Kanda, K.; Endo, K.; Yonezawa, T. *J. Am. Chem. Soc.* **1984**, *106*, 4653−4660.
(25) Kitagawa, S.; Munakata, M.; Sasaki, M. *Inorg. Chim. Acta* **1986**, *120*, 77−80.
(26) Endo, K.; Yamamoto, K.; Deguchi, K.; Matsushita, K. *Bull. Chem. Soc. Jpn.* **1987**, *60*, 2803−2807.
(27) Mohr, B.; Brooks, E. E.; Rath, N.; Deutsch, E. *Inorg. Chem.* **1991**, *30*, 4541−4545.
(28) Gill, D. S. *J. Chem. Soc., Faraday Trans.* **1995**, *91*, 2307−2312.
(29) Black, J. R.; Champness, N. R.; Levason, W.; Reid, G. *Inorg. Chem.* **1996**, *35*, 1820−1824.
(30) Imai, S.; Fujisawa, K.; Kobayashi, T.; Shirasawa, N.; Fujii, H.; Yoshimura, T.; Kitajima, N.; Moro-oka, Y. *Inorg. Chem.* **1998**, *37*, 3066−3070.
(31) Kroeker, S.; Wasylishen, R. E.; Hanna, J. V. *J. Am. Chem. Soc.* **1999**, *121*, 1582−1590.
(32) Irangu, J. K.; Jordan, R. B. *Inorg. Chem.* **2003**, *42*, 3934−3942.

Experimental Section

General Methods. The manipulation of copper(I) complexes was performed under an Ar atmosphere using standard Schlenk techniques and an inert-atmosphere glovebox. Anhydrous solvents were purchased from commercial sources and were degassed before use. The tridentate ligands, 3,5-*i*Pr$_2$-TPB,[33] *i*Pr-TIC,[34] Ph-TIC,[34] 3,5-*i*Pr$_2$-TPM,[35] 3,5-Me$_2$-TPM,[36] TPC,[37] TPME,[38] TPYM,[39] Me-TACN,[40] *i*Pr-TACN,[41] Bn-TACN,[42] and Me-TACD,[43] were synthesized as described previously. Synthesis of *i*Pr-BITC will be published elsewhere. The metal complexes, [(CH$_3$CN)$_4$Cu]ClO$_4$,[44] (3,5-*i*Pr$_2$-TPB)Cu,[33] (3,5-*i*Pr$_2$-TPB)Cu(CH$_3$CN),[35] (3,5-*i*Pr$_2$-TPB)-Cu(PPh$_3$),[33] [(3,5-*i*Pr$_2$-TPM)Cu(CH$_3$CN)]ClO$_4$,[35] [(3,5-*i*Pr$_2$-TPM)-CuCO]ClO$_4$,[35] [(*i*Pr-TACN)Cu(CH$_3$CN)]ClO$_4$,[45] and [(Bn-TACN)-CuCO]ClO$_4$,[45] were prepared by a previously published method. All other reagents were obtained from commercial sources and used as received.

Safety Note. Caution! *Although we have not encountered any problems, it should be noted that perchlorate complexes are potentially explosive and should be handled with great care.*

Synthesis of 3,5-Ph$_2$-TPM. 3,5-Ph$_2$-TPM was synthesized by the same procedure as was used for 3,5-Me$_2$-TPM using 3,5-diphenylimidazole as a starting material in 37% yield. ^{1}H NMR (CDCl$_3$): δ 7.82 (1H, s), 7.80 (6H, d, J = 7.0 Hz), 7.34 (6H, t, J = 7.5 Hz), 7.29−7.22 (6H, m), 7.14 (6H, t, J = 7.7 Hz), 6.81 (6H, d, J = 7.1 Hz), 6.57 (3H, s). ^{13}C NMR (CDCl$_3$): δ 151.5, 145.2, 133.1, 129.3, 129.0, 128.8, 128.5, 128.4, 128.2, 128.1, 126.3, 126.0, 105.3, 105.0. IR (KBr, cm^{-1}): 3056, 1604, 1559, 1484, 1460, 1436, 1407, 1321, 1300, 1275, 1212, 1082, 1026, 1006, 954, 917, 835, 809, 759, 691, 579.

Synthesis of Et-TIC. Et-TIC was synthesized by the same procedure for *i*Pr-TIC and Ph-TIC using 2-ethylimidazole as a starting material in 15% yield. ^{1}H NMR (CDCl$_3$): δ 6.76 (3H, s), 3.98 (1H, br), 3.46 (9H, s), 2.64 (6H, q, J = 7.8 Hz), 1.20 (9H, t, J = 7.6 Hz). ^{13}C NMR (CDCl$_3$): δ 147.4, 143.7, 117.3, 69.8, 31.4, 19.4, 11.9. IR (KBr, cm^{-1}): 3368, 2977, 2935, 2874, 1559, 1506, 1470, 1410, 1375, 1292, 1169, 1073, 1028, 971, 887.

Preparation for Copper(I) Acetonitrile Complexes. Typical procedure: To a solution of the desired tridentate ligand in THF was added 1 equiv of solid [Cu(CH$_3$CN)$_4$]ClO$_4$. The resulting mixture was stirred for several hours at ambient temperature and then filtered. Pentane was added to the filtrate with rapid stirring, causing the precipitation of the copper(I) acetonitrile complex as a colorless powder. The copper acetonitrile complex was further purified by re-crystallization from CH$_3$CN/Et$_2$O. Exceptionally, [(Et-TIC)Cu(CH$_3$CN)]ClO$_4$, [(TPME)Cu(CH$_3$CN)]ClO$_4$, [(TPYM)Cu(CH$_3$-CN)]ClO$_4$, and [(*i*Pr-BITC)Cu(CH$_3$CN)]ClO$_4$ were used for the preparation of carbonyl complexes without characterization. [(3,5-Me$_2$-TPM)Cu(CH$_3$CN)]ClO$_4$. ^{1}H NMR (CD$_2$Cl$_2$): δ 7.77 (1H, s), 6.08 (3H, s), 2.60 (9H, s), 2.38 (9H, s), 1.99 (3H, s). IR (KBr, cm^{-1}): 3091, 2994, 2949, 2919, 2253, 1568, 1466, 1415, 1394, 1306, 1247, 1088, 1036, 974, 902, 853, 827, 812, 792, 707, 625, 480. [(3,5-Ph$_2$-TPM)Cu(CH$_3$CN)]ClO$_4$. ^{1}H NMR (CD$_2$Cl$_2$): δ 8.46 (1H, s), 8.00 (6H, d, J = 6.6 Hz), 7.63−7.61 (9H, m), 7.55 (3H, t, J = 7.6 Hz), 7.23 (6H, t, J = 7.9 Hz), 7.07 (6H, d, J = 8.2 Hz), 6.86 (3H, s), 2.16 (3H, s). IR (KBr, cm^{-1}): 3127, 3099, 3061, 2927, 2292, 1638, 1558, 1486, 1460, 1438, 1412, 1371, 1269, 1215, 1152, 1077, 1030, 1005, 959, 925, 849, 824, 761, 701, 667, 636, 580, 517. [(TPC)Cu(CH$_3$CN)]ClO$_4$. ^{1}H NMR (CD$_3$CN): δ 8.62 (3H, d, J = 4.9 Hz), 8.09 (3H, d, J = 8.2 Hz), 7.94 (3H, d, J = 8.0 Hz), 7.40 (3H, d, J = 7.7 Hz), 5.94 (1H, s), 2.14 (3H, s). IR (KBr, cm^{-1}): 3082, 2275, 1593, 1464, 1437, 1364, 1308, 1287, 1188, 1158, 1148, 1118, 1055, 932, 887, 776, 755, 660, 623, 517, 502. [(Me-TACN)Cu(CH$_3$CN)]ClO$_4$. ^{1}H NMR (CD$_3$CN): δ 2.64 (6H, m), 2.62 (9H, s), 2.10 (3H, s). IR (KBr, cm^{-1}): 2947, 2882, 2819, 2252, 1493, 1455, 1362, 1300, 1253, 1216, 1092, 1020, 982, 941, 891, 770, 744, 625, 570, 494. [(Me-TACD)Cu(CH$_3$CN)]ClO$_4$. ^{1}H NMR (CD$_3$CN): 2.73−2.68 (6H, m), 2.51−2.46 (6H, m), 2.41 (9H, s), 1.95 (3H, s), 1.85−1.72 (6H, m).

Preparation of Copper(I) Carbonyl Complexes. Typical procedure: The copper(I) acetonitrile complex was dissolved in a minimum amount of CH$_2$Cl$_2$. The CH$_2$Cl$_2$ solution was stirred under an atmosphere of CO for 1 h at ambient temperature. The diffusion of Et$_2$O into the solution resulted in the crystallization of the product as a colorless solid. Because of its instability, [(*i*Pr-BITC)CuCO]-ClO$_4$ was not isolated as a solid and used without crystallization. [(3,5-Me$_2$-TPM)CuCO]ClO$_4$. Yield: 73%. ^{1}H NMR (CD$_2$Cl$_2$): δ 7.87 (1H, s), 6.16 (3H, s), 2.67 (9H, s), 2.44 (9H, s). IR (KBr, cm^{-1}): 3141, 2989, 2929, 2111, 1560, 1465, 1400, 1303, 1252, 1092, 1043, 981, 907, 854, 780, 703, 663, 624. [(3,5-Ph$_2$-TPM)-CuCO]ClO$_4$. Yield: 79%. ^{1}H NMR (CD$_2$Cl$_2$): δ 8.51 (1H, s), 7.87 (6H, br), 7.67−7.59 (12H, m), 7.26−7.07 (12H, m), 6.88 (3H, s). IR (KBr, cm^{-1}): 3124, 3058, 2927, 2108, 1556, 1485, 1460, 1438, 1413, 1372, 1322, 1275, 1254, 1203, 1179, 1103, 1027, 1007, 960, 924, 841, 826, 811, 775, 758, 700, 623, 580. Anal. Calcd for C$_{47.5}$H$_{35}$N$_6$Cl$_2$CuO$_5$ ([(3,5-Ph$_2$-TPM)CuCO]ClO$_4$·0.5CH$_2$Cl$_2$): C, 63.09; H, 3.90; N, 9.29. Found: C, 62.64; H, 4.21; N, 9.75. [(Et-TIC)CuCO]ClO$_4$. Yield: 58%. ^{1}H NMR (CD$_2$Cl$_2$): δ 7.09 (3H, s), 5.11 (1H, br), 3.64 (9H, s), 2.87 (6H, q, J = 7.0 Hz), 1.36 (9H, d, J = 7.1 Hz). IR (KBr, cm^{-1}): 3449, 2974, 2942, 2877, 2076, 1483, 1457, 1415, 1379, 1318, 1291, 1201, 1112, 1070, 932, 889, 779, 737, 625. Anal. Calcd for C$_{23.3}$H$_{34.6}$N$_6$Cl$_{1.6}$CuO$_6$ ([(Et-TIC)-CuCO]ClO$_4$·0.3CH$_2$Cl$_2$): C, 45.50; H, 5.67; N, 13.66. Found: C, 45.55; H, 5.82; N, 13.33. [(*i*Pr-TIC)CuCO]ClO$_4$. Yield: 67%. ^{1}H NMR (CD$_2$Cl$_2$): δ 7.07 (3H, s), 5.21 (1H, br), 3.65 (9H, s), 3.28 (3H, sept, J = 7.0 Hz), 1.51 (18H, d, J = 7.1 Hz). IR (KBr, cm^{-1}): 2970, 2930, 2872, 2069, 1483, 1421, 1383, 1362, 1310, 1283, 1089, 930, 902, 874, 844, 768. [(Ph-TIC)CuCO]ClO$_4$. Yield: 69%. ^{1}H NMR (CD$_2$Cl$_2$): δ 7.53−7.48 (15H, m), 7.34 (3H, s), 5.32 (1H, s), 3.65 (9H, s). IR (KBr, cm^{-1}): 3411, 3162, 3125, 3070, 2954, 2076, 1579, 1474, 1440, 1403, 1366, 1317, 1291, 1239, 1186, 1105, 1021, 931, 921, 883, 781, 739, 713, 701, 677, 658, 624, 559. [(TPYM)CuCO]ClO$_4$. Yield: 45%. ^{1}H NMR (CD$_2$Cl$_2$): δ 8.79 (3H, d, J = 4.7 Hz), 8.18 (3H, d, J = 7.6 Hz), 8.04 (3H, t, J = 7.7 Hz), 7.51 (3H, t, J = 6.4 Hz), 6.47 (1H, s). IR (KBr, cm^{-1}): 3073, 2976, 2091, 1600, 1577, 1474, 1442, 1355, 1159, 1089,1025, 912,

(33) Kitajima, N.; Fujisawa, K.; Fujimoto, C.; Moro-oka, Y.; Hashimoto, S.; Kitagawa, T.; Toriumi, K.; Tatsumi, K.; Nakamura, A. *J. Am. Chem. Soc.* **1992**, *114*, 1277−1291.

(34) Kujime, M.; Fujii, H. *Tetrahedron Lett.* **2005**, *46*, 2809−2812.

(35) Fujisawa, K.; Ono, T.; Ishikawa, Y.; Amir, N.; Miyashita, Y.; Okamoto, K.; Lehnert, N. *Inorg. Chem.* **2006**, *45*, 1698−1713.

(36) Juliá, S.; del Mazo, J.; Avila, L. *Org. Prep. Proced. Int.* **1984**, *16*, 299−307.

(37) Wibaut, J. P.; de Jonge, A. P.; Van der Voort, H. G. P.; Otto, H. L. *Recl. Trav. Chim. Pays-Bas* **1951**, *70*, 1054−1066.

(38) Jonas, R. T.; Stack, T. D. P. *Inorg. Chem.* **1998**, *37*, 6615−6629.

(39) White, D. L.; Faller, J. W. *Inorg. Chem.* **1982**, *21*, 3119−3122.

(40) Wieghardt, K.; Chaudhuri, P.; Nuber, B.; Weiss, J. *Inorg. Chem.* **1982**, *21*, 3086−3090.

(41) Haselhorst, G.; Stoetzel, S.; Strassburger, A.; Walz, W.; Wieghardt, K.; Nuber, B. *J. Chem. Soc., Dalton Trans.* **1993**, 83−90.

(42) Beissel, T.; Della Vedova, B. S. P. C.; Wieghardt, K.; Boese, R. *Inorg. Chem.* **1990**, *29*, 1736−1741.

(43) Kallinen, K. O.; Pakkanen, T. T.; Pakkanen, T. A. *J. Organomet. Chem.* **1997**, *547*, 319−327.

(44) Hathaway, B. J.; Holah, D. G.; Postlethwaite, J. D. *J. Chem. Soc.* **1961**, 3215.

(45) Mahapatra, S.; Halfen, J. A.; Wilkinson, E. C.; Pan, G.; Wang, X.; Young, V. G., Jr.; Cramer, C. J.; Que, L., Jr.; Tolman, W. B. *J. Am. Chem. Soc.* **1996**, *118*, 11555−11574.

Table 1. Crystallographic Data for [(*i*Pr-TIC)CuCO]ClO_4, [(Me-TACN)CuCO]ClO_4, and [(Bn-TACN)CuCO]ClO_4

	[(*i*Pr-TIC)CuCO]ClO_4·$2CH_2Cl_2$	[(Me-TACN)CuCO]ClO_4	[(Bn-TACN)CuCO]ClO_4
empirical formula	$C_{25}H_{38}N_6Cl_5O_6Cu$	$C_{10}H_{21}N_3ClO_5Cu$	$C_{22}H_{33}N_3ClO_5Cu$
crystal system	orthorhombic	cubic	orthorhombic
mol wt	759.42	362.29	518.52
space group	$P2_12_12_1$	$P213$	*Pbca*
a, Å	17.289(2)	11.3362(1)	16.205(3)
b, Å	22.316(4)	11.3362(1)	17.827(3)
c, Å	8.866(1)	11.3362(1)	18.731(3)
V, Å^3	3420(6)	1456.8(2)	5411(1)
Z	4	4	8
D_{calcd}, g cm^{-3}	1.475	1.652	1.273
μ(Mo Kα), cm^{-1}	10.74	17.04	9.39
temperature, °C	−100	−100	−100
no. of observations	3322 (all data)	1101	6191 (all data)
no. of variables	390	62	343
R1, %	4.3	2.0	8.9
wR2, %	11.3	5.2	16.9

882, 850, 783, 762, 739, 648, 622, 503. [(TPC)CuCO]ClO_4. Yield: 72%. ^{1}H NMR (CD_2Cl_2): δ 8.78 (3H, d, J = 4.6 Hz), 8.48 (3H, d, J = 8.3 Hz), 8.11 (3H, t, J = 7.9 Hz), 7.52 (3H, t, J = 6.1 Hz), 6.87 (1H, s). IR (KBr, cm^{-1}): 3083, 2102, 1596, 1465, 1438, 1311, 1290, 1189, 1156, 1120, 1050, 929, 890, 774, 756, 660. [(TPME)CuCO]ClO_4. Yield: 61%. ^{1}H NMR (CD_2Cl_2): δ 8.83 (3H, d, J = 5.2 Hz), 8.16−8.11 (6H, m), 7.59−7.56 (3H, m), 7.52 (3H, t, J = 6.1 Hz), 3.99 (3H, s). IR (KBr, cm^{-1}): 3120, 3071, 2989, 2101, 1594, 1466, 1437, 1311, 1296, 1203, 1092, 1020, 979, 939, 775, 760, 672, 659, 641, 623, 524, 506. [(Me-TACN)CuCO]ClO_4. Yield: 71%. ^{1}H NMR (CD_2Cl_2): δ 2.99 (9H, s), 2.98(6H, m). IR (KBr, cm^{-1}): 2988, 2972, 2943, 2862, 2825, 2081, 1490, 1474, 1433, 1426, 1362, 1301, 1214, 1165, 1090, 1015, 986, 891, 776, 747, 623, 573. [(*i*Pr-TACN)CuCO]ClO_4. Yield: 57%. ^{1}H NMR (CD_2Cl_2): δ 3.33 (3H, sept, J = 6.5 Hz), 3.05−2.99 (6H, m), 2.88−2.83 (6H, m), 1.36 (18H, d, J = 6.6 Hz). IR (KBr, cm^{-1}): 2969, 2937, 2871, 2084, 2062, 1489, 1470, 1455, 1394, 1380, 1373, 1348, 1335, 1325, 1276, 1160, 1137, 1092, 1006, 962, 950, 841, 775, 721, 623. [(Me-TACD)CuCO])ClO_4. Yield: 65%. ^{1}H NMR (CD_2Cl_2): δ 2.94−2.89 (6H, m), 2.74−2.69 (6H, m), 2.71 (9H, s), 2.16−2.09 (3H, m), 2.06−1.99 (3H, m). IR (KBr, cm^{-1}): 2926, 2871, 2070, 1473, 1317, 1285, 1210, 1175, 1092, 1023, 976, 904, 874, 794, 744, 726, 622. [(*i*Pr-BITC)CuCO])ClO_4. Yield: 55%. ^{1}H NMR (CD_2Cl_2): δ 7.32−7.28 (5H, m), 7.25 (2H, s), 7.05 (2H, d, J = 7.3 Hz), 5.16 (1H, br), 3.73 (6H, s), 3.61 (2H, s), 3.24 (2H, hept, J = 7.0 Hz), 1.43 (6H, d, J = 7.0 Hz), 1.29 (6H, d, J = 7.0 Hz). IR (in CH_2Cl_2, cm^{-1}): 2093.

Preparation of ^{13}C Enriched Copper Carbonyl Complexes. The ^{13}C-labeled compounds of copper carbonyl complexes were prepared in a similar manner as described above, except ^{13}C-labeled carbon monoxide was used. The preparations were carried out in NMR tubes, and the products were used without further purification. The clean formation of the desired copper(I) carbonyl complex was confirmed by comparison of its ^{1}H NMR spectrum with that of a non-labeled sample.

Instruments. NMR spectra were recorded on a JEOL JNM-LA500 spectrometer. ^{13}C NMR spectra were obtained at sweep-widths of 34 kHz at 125.78 MHz using 32K data points. ^{63}Cu NMR spectra were obtained at sweep-widths of 200 kHz at 132.66 MHz using 16K data points. The pulse repetition time and pulse width were 0.1 s and 9 μs, respectively. Typically, 20 000 transients were collected for all copper(I) complexes. The sample concentrations of the copper(I) complexes were ~20 mM. The chemical shift values of ^{13}C and ^{63}Cu NMR spectra are referenced to external tetramethylsilane (TMS) in chloroform and tetrakis(acetonitrile)-copper(I) haxafluorophosphate, [$(CH_3CN)_4Cu$]PF_6, in acetonitrile-d_3, respectively. FT-IR spectra were obtained using a JASCO FT/IR-460 spectrometer, as KBr pellets. The accuracy of frequency for the IR bands was ±1 cm^{-1}. Elemental analyses were performed at the Research Center for Molecular-Scale Nanoscience, Institute for Molecular Science.

X-ray Data Collection. Crystallographic data and the results of refinements are summarized in Table 1. Diffraction measurements for the single crystals of [(*i*Pr-TIC)CuCO]ClO_4, [(Me-TACN)-CuCO]ClO_4, and [(Bn-TACN)CuCO]ClO_4 were made using Mo Kα radiation (λ = 0.71070 Å) on a Rigaku RAXIS IV imaging plate area detector or Rigaku MSC mercury charge coupled device at 173 K. The data were corrected for Lorentz polarization effects. Empirical absorption corrections were applied. The structural analysis was performed using the teXsan crystallographic software package.[46] The structures were solved by a combination of direct method (SIR92)[47] and Fourier synthesis (DIRDIF94).[48] Least-squares refinements were carried out using teXsan or SHELXL-97.[49] All non-hydrogen atoms were refined anisotropically. Hydrogen atoms were placed at the calculated positions except for the O−H moiety in [(*i*Pr-TIC)CuCO]ClO_4.

Results

Crystal Structures of Copper(I) Carbonyl Complexes. The crystal structures of [(*i*Pr-TIC)CuCO]ClO_4, [(Me-TACN)CuCO]ClO_4, and [(Bn-TACN)CuCO]ClO_4 were determined by X-ray crystallography (Figure 2 and Table 1), and the selected bond distances and angles are listed in Table 2. These complexes have a distorted tetrahedral geometry around the copper ion. The coordination structures of these copper(I) carbonyl complexes are very close to those of the corresponding acetonitrile complexes reported previously.[34,50] The copper bound CO does not induce any significant structural change around the copper ion. To investigate the effect of tridentate ligands on their structure, we further compared these complexes to other copper(I) carbonyl

(46) *teXsan*; *Crystal Structure Analysis Package*, version 1.11; Rigaku Corp.: Tokyo, Japan, 2000.
(47) Altomare, A.; Cascarano, G.; Giacovazzo, C.; Guagliardi, A.; Burla, M. C.; Polidoli, G.; Camalli, M. *J. Appl. Crystallogr.* **1994**, *27*, 435.
(48) Beurskens, P. T.; Admiraal, G.; Beurskens, G.; Bosman, W. P.; de Gelder, R.; Israel, R.; Smits, J. M. M. *The DIRDIF-94 Program System*; Technical Report for the Crystallography Laboratory; University of Nijmegen: Nijmegen, The Netherlands, 1994.
(49) Sheldrick, G. M. *SHELXL-97*: *Program for Crystal Structure Refinement;* University of Göttingen: Göttingen, Germany, 1997.
(50) Lam, B. M. T.; Halfen, J. A.; Young, V. G., Jr.; Hagadorn, J. R.; Holland, P. L.; Cucurull-Sánchez, L.; Novoa, J. J.; Alvarez, S.; Tolman, W. B. *Inorg. Chem.* **2000**, *39*, 4059−4072.

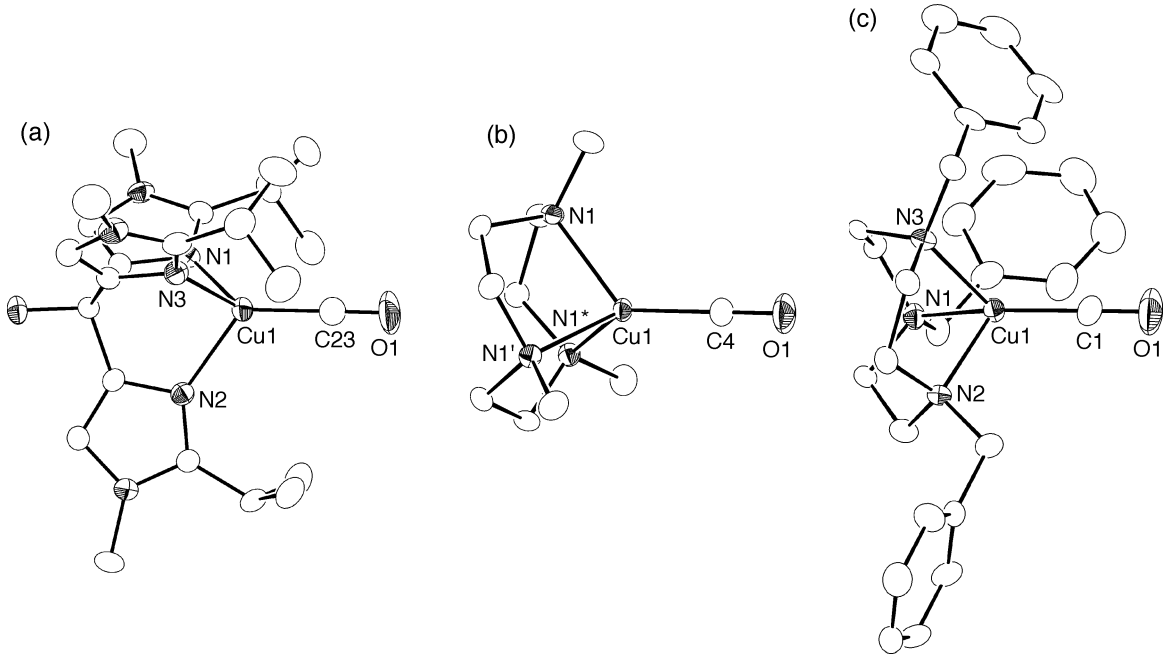

Figure 2. ORTEP drawing of (a) [(*i*Pr-TIC)CuCO]ClO_4, (b) [(Me-TACN)CuCO]ClO_4, and (c) [(Bn-TACN)CuCO]ClO_4 with thermal ellipsoids at the 50% probability level.

Table 2. Selected Bond Lengths (Å) and Angles (deg) for Copper(I) Carbonyl Complexes

complex	Cu−C	C−O	Cu−N (av)	Cu−C−O	N−Cu−C (av)	N−Cu−N (av)	ref
(3,5-*i*Pr$_2$-TPB)CuCO	1.769(8)	1.118(10)	2.018(4)	178.6(9)	124.7(4)	90.8(9)	33
(3-*t*Bu-5-Me-TPB)CuCO	1.797(11)	1.110(6)	2.062(5)	177.6(6)	123.3(18)	92.7(9)	30
(3-*t*Bu-5-*i*Pr-TPB)CuCO	1.76(1)	1.14(1)	2.059(1)	178(1)	123.2(2)	92.9(8)	35
(3,5-Ph$_2$-TPB)CuCO	1.78(1)	1.08(1)	2.059(6)	180.0(1)	125.0(2)	90.4(2)	30
[(3,5-*i*Pr$_2$-TPM)CuCO]ClO_4	1.777(5)	1.127(6)	2.041(10)	175.6(6)	126.7(3)	87.9(14)	35
[(*i*Pr-TIC)CuCO]ClO_4	1.783(6)	1.130(7)	2.075(4)	176.7(7)	124.9(2)	90.5(2)	this work
[(Me-TACN)CuCO]ClO_4	1.778(3)	1.127(4)	2.092(13)	180.0(4)	128.24(4)	85.72(6)	this work
[(Bn-TACN)CuCO]ClO_4	1.771(6)	1.130(7)	2.097(5)	177.7(6)	127.5(2)	86.3(2)	this work

complexes with tridentate ligands, such as (3,5-*i*Pr$_2$-TPB)-CuCO,[33] (3-*t*Bu-5-Me-TPB)CuCO,[30] (3,5-Ph-TPB)CuCO,[30] and [(3,5-*i*Pr$_2$-TPM)CuCO]ClO_4.[35] As shown in Table 2, no significant change in the Cu−C and C−O bond lengths or the Cu−C−O angles were found for these copper carbonyl complexes. However, the bond lengths between the copper ion and the N atoms of the tridentate ligand, Cu−N, were changed slightly, depending on the tridentate ligand. The Cu−N bond lengths for complexes with imino tridentate ligands (TPB, TPM, and TIC) are shorter than those with the amino tridentate ligands (TACN). The average Cu−N bond lengths for the TPB derivatives are the shortest in these complexes because TPB ligands with a negative charge can bind positively charged copper(I) ion stronger than neutral ligands such as TPM and TIC.

IR Spectroscopy of Copper(I) Carbonyl Complexes. The IR spectra of the copper(I) carbonyl complexes showed intense absorptions in the range of 2050−2200 cm^{-1}, corresponding to stretching vibrations of a copper bound CO, ν(C≡O), which is sensitive to copper−CO bond character.[51,52] To investigate the electronic effect of a tridentate ligand on the Cu−CO moiety, we obtained infrared spectra of copper(I) carbonyl complexes, and the ν(C≡O) values for copper(I) carbonyl complexes are summarized in Table 3. As shown in Table 3, the ν(C≡O) values for copper(I) carbonyl complexes are sensitive to the tridentate ligand. For [(*i*Pr-TACN)CuCO]ClO_4, a main ν(C≡O) band at 2062 cm^{-1} with a shoulder band at 2084 cm^{-1} was found in the solid state (KBr pellet), but only a 2082 cm^{-1} band in dichloromethane solution was observed (see Figure S1, Supporting Information).[53] The lower wavenumber band at 2062 cm^{-1} was consistent with a previous report for [(*i*Pr-TACN)CuCO]-SbF_6 (2067 cm^{-1}) in a solid state (KBr pellet).[45] The ν(C≡O) values for the tridentate ligands were increased roughly in the order of hydrotris(pyrazolyl)borate (TPB) < tris(4-imidazolyl)carbinol (TIC) < triazacyclododecacene (TACD) < triazacyclononane (TACN) < tris(pyridyl)carbinol (TPC) < tris(pyrazolyl)methane (TPM). Contrarily, this indicates that the π back-donation to the copper bound CO is decreased in this order. The ν(C≡O) values are also changed by the substituents of the ligand. Interestingly, the ν(C≡O) values for the complexes containing tridentate

(51) Strauss, S. H. *J. Chem. Soc., Dalton Trans.* **2000**, 1−6.
(52) Willner, H.; Aubke, F. *Angew. Chem., Int. Ed.* **1997**, *36*, 2402−2425.

(53) Ratio of the signal intensities of 2062 and 2084 cm^{-1} bands was changed by preparations. Although we do not have definite assignments for these two bands, these two bands may be caused by a conformational change of the isopropyl substituents in a solid state. For example, content of solvent molecule in a microcrystal may change a ratio of the conformational isomers.

Table 3. Vibrational Data and ^{63}Cu and ^{13}C NMR Chemical Shifts of Copper(I) Complexes

complex	ν(C≡O)[a], cm^{-1}	δ (^{63}Cu NMR),[b] ppm (line width $W_{1/2}$, Hz)		δ (^{13}C NMR),[b] ppm
(3,5-*i*Pr$_2$-TPB)CuCO	2061[c,j]	730	(205)[d,h]	177.2[g]
(3,5-*i*Pr$_2$-TPB)Cu(CH$_3$CN)		166	(12000)[e]	
(3,5-*i*Pr$_2$-TPB)Cu(PPh$_3$)		118	(11000)[e]	
(3-*t*Bu-5-Me-TPB)CuCO	2064[c,j]	700	(70)[d,h]	
(3,5-Me$_2$-TPB)CuCO	2062[c,j]	716	(110)[d,h]	
(3-*t*Bu-5-*i*Pr-TPB)CuCO	2064[c,j]	703	(75)[d,h]	174.0[h,k]
(3-Ph-5-*i*Pr-TPB)CuCO	2077[c,j]	603	(2900)[d,h]	
(3,5-Ph$_2$-TPB)CuCO	2079[c,j]	585	(4200)[d,h]	
[(3,5-*i*Pr$_2$-TPM)CuCO]ClO$_4$	2102	449	(8200)	174.7
[(3,5-*i*Pr$_2$-TPM)Cu(CH$_3$CN)]ClO$_4$		113	(9700)[e]	
[(3,5-Me$_2$-TPM)CuCO]ClO$_4$	2111	419	(4700)	
[(3,5-Ph$_2$-TPM)CuCO]ClO$_4$	2108	440	(12000)	
[(*i*Pr-TIC)CuCO]ClO$_4$	2069	621	(1800)	173.5
[(*i*Pr-TIC)Cu(CH$_3$CN)]ClO$_4$		N.D.	v.b.[e]	
[(Et-TIC)CuCO]ClO$_4$	2076	609	(1300)	
[(Ph-TIC)CuCO]ClO$_4$	2080	543	(4500)	
[(TPC)CuCO]ClO$_4$	2106	504	(6600)	174.4
[(TPC)Cu(CH$_3$CN)]ClO$_4$		N.D.	v.b.[e]	
[(TPCME)CuCO]ClO$_4$	2102	524	(8700)	
[(TPYM)CuCO]ClO$_4$	2091	489	(6500)	
[(*i*Pr-TACN)CuCO]ClO$_4$	2062(2084)	461	(5500)	
[(*i*Pr-TACN)Cu(CH$_3$CN)]ClO$_4$		−62	(14000)[e]	
[(Me-TACN)CuCO]ClO$_4$	2081	419	(4100)	
[(Bn-TACN)CuCO]ClO$_4$	2083	394	(14000)	175.2
[(Me-TACD)CuCO]ClO$_4$	2070	585	(410)	173.3[f,i]
[(Me-TACD)Cu(CH$_3$CN)]ClO$_4$		−83	(6600)[e]	
[(*i*Pr-BITC)CuCO]ClO$_4$	2093[b]	451	(10000)	

[a] As KBr pellets. [b] In dichloromethane-d_2. [c] In toluene. [d] In toluene-d_8. [e] In acetonitrile-d_3. [f] In 1,2-dichloroethane-d_2. [g] Quartet, J = 663 Hz. [h] Quartet, J = 655 Hz (in chloroform-*d*). [i] Quartet, J = 586 Hz. [j] Reference 30. [k] Reference 35.

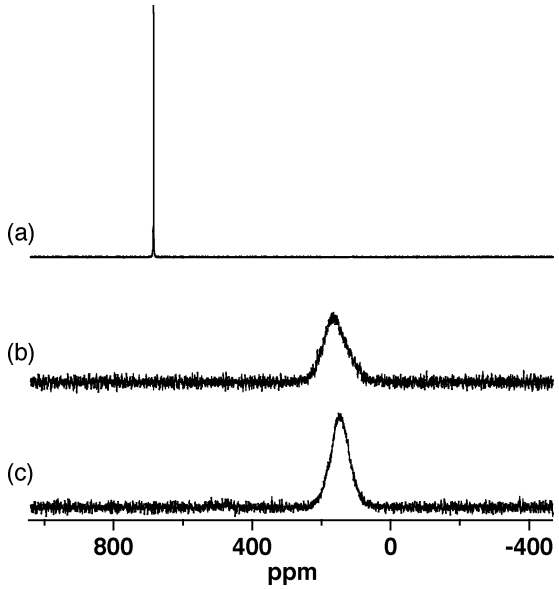

Figure 3. ^{63}Cu NMR spectra of (a) (3,5-*i*Pr$_2$-TPB)CuCO in CD_2Cl_2, (b) (3,5-*i*Pr$_2$-TPB)Cu(CH$_3$CN) in CD_3CN, and (c) (3,5-*i*Pr$_2$-TPB)Cu(PPh$_3$) in CD_3CN at 298 K.

ligands with isopropyl substituents (3,5-*i*Pr$_2$-TPB, *i*Pr-TPM, *i*Pr-TIC, and *i*Pr-TACN) were smaller than those with other substituents.

^{63}Cu NMR Spectroscopy of Copper(I) Complexes. As reported previously, the ^{63}Cu NMR spectra of copper(I) carbonyl complexes with TPB ligands exhibited very sharp signals at around 600−700 ppm.[30] To investigate the effect of the fourth ligand on the ^{63}Cu NMR signal, we obtained ^{63}Cu NMR spectra of copper(I) 3,5-*i*Pr$_2$-TPB complexes with various fourth ligands. As shown in Figure 3, while an extremely sharp ^{63}Cu NMR signal is observed for the carbonyl complex, the ^{63}Cu NMR signals for the acetonitrile and triphenylphosphine complexes are quite broad. Furthermore, the carbonyl complex shows a large downfield shift of the ^{63}Cu NMR signal, but the acetonitrile and triphenylphosphine complexes do not.

Similar results were obtained for other tridentate ligands. The ^{63}Cu NMR signals for copper(I) acetonitrile complexes with other tridentate ligands were also extremely broad or undetectable and did not show a large downfield shift (Table 3). On the other hand, for most copper(I) carbonyl complexes, the ^{63}Cu NMR signals become significantly sharper and are shifted far downfield, to around 400−800 ppm (Figure 4 and Table 3).

To determine if the line width variations might be due to differences in relaxation mechanisms, we examined the temperature dependence of ^{63}Cu NMR signals for copper(I) complexes with various tridentate ligands. As shown in Figure 5, the ^{63}Cu NMR signals for all of these copper(I) complexes become sharper with increasing temperature.[54,55] This is in contrast to previous ^{63}Cu NMR studies of tetrahedral copper(I) acetonitrile and phosphite complexes, $[(CH_3CN)_4Cu]^+$ and $[(P(OR)_3)_4Cu]^+$, whose line widths were increased with increasing temperature.[20,32] Although the previous results could be interpreted to be due to a ligand exchange process, the present results are consistent to a quadrupole relaxation mechanism, for which the line width of the ^{63}Cu NMR signal is decreased with increasing temperature. To further confirm the quadrupole relaxation

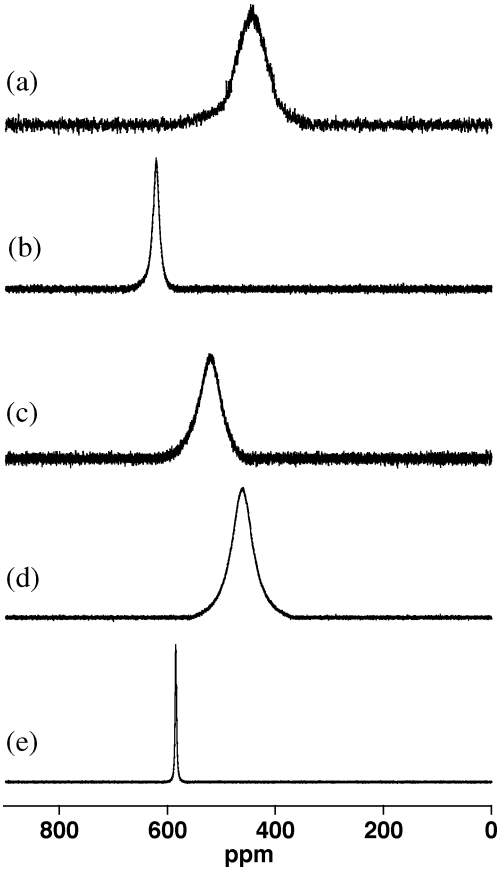

Figure 4. ^{63}Cu NMR spectra of copper(I) carbonyl complexes, (*i*Pr-TPMCuCO)ClO_4 (a), (*i*Pr-TICCuCO)ClO_4 (b), (TPCCuCO)ClO_4 (c), (Me-TACNCuCO)ClO_4 (d), and (Me-TACDCuCO)ClO_4 (e), in CD_2Cl_2 at 298 K.

mechanism for these copper(I) complexes with various tridentate ligands, the temperature dependence of the line widths are simulated with the quadrupole relaxation rate, given by eq 1

$$\frac{1}{T_2} = \pi W_{1/2} = \frac{3(2I+1)}{40\{I^2(2I-1)\}}\left(1+\frac{\eta^2}{3}\right)\left(\frac{2\pi e^2 qQ}{h}\right)^2 \tau_Q = 3.9478(\mathrm{QCC})^2\tau_Q \quad (1)$$

where $W_{1/2}$ is the line width at half-height, η is the symmetry parameter, τ_Q is the correlation time, and (QCC) is an effective quadrupole coupling constant. From the Stokes−Einstein relationship, the correlation time can be expressed as $\tau_Q \propto \eta_{sample}/T$, where η_{sample} is the viscosity of the sample and T is temperature of the sample. At low concentration, the viscosity of the sample is very close to the viscosity of the solvent ($\eta_{solvent}$), $\eta_{sample} \approx \eta_{solvent}$, and $\eta_{solvent}$ is given by $\eta_{solvent} \propto \exp(E_a/RT)$, where E_a is the activation energy for

(54) ^{63}Cu NMR signals for copper(I) complexes slightly shifted upfield with increasing temperature (see Supporting Information). Similar upfield shifts were also reported in previous studies (e.g., ref 20). As discussed in previous studies, interpretation of such temperature dependence may be complicated by the lack of a suitable internal reference, which would allow the temperature-induced changes in bulk magnetic susceptibility to be accounted. On the other hand, the strength of the Cu−CO bond would not be changed by temperature because the ν(C≡O) value for (3,5-*i*Pr$_2$-TPB)CuCO at 353 K was the same as that at 298 K.

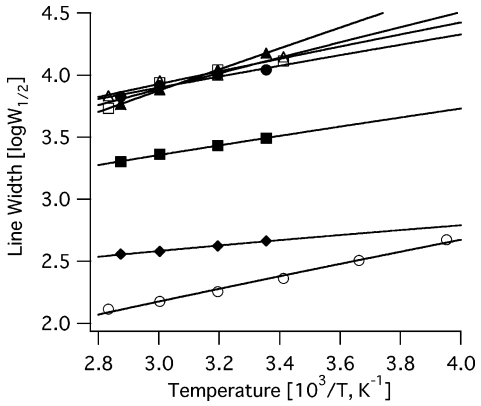

Figure 5. Temperature dependent ^{63}Cu NMR line widths for copper(I) complexes. The solid lines show least-square fits by eq 2. These data are summarized in Table S1, Supporting Information. ○, (3,5-*i*Pr$_2$-TPB)CuCO in toluene-d_8; □, (3,5-*i*Pr$_2$-TPB)Cu(CH_3CN) in toluene-d_8; △, (3,5-*i*Pr$_2$-TPB)Cu(PPh_3) in toluene-d_8; ●, [(3,5-*i*Pr$_2$-TPB)CuCO]ClO_4 in 1,2-$C_2D_4Cl_2$; ■, [(*i*Pr-TIC)CuCO]ClO_4 in 1,2-$C_2D_4Cl_2$; ▲, [(*i*Pr-TACN)CuCO]ClO_4 in C_6D_5Cl; ◆, [(Me-TACD)CuCO]ClO_4 in 1,2-$C_2D_4Cl_2$.

re-orientation of the copper complex. Therefore, eq 1 is simplified to eq 2.

$$W_{1/2} = A\frac{\exp(E_a/RT)}{T} \quad (2)$$

where A is a proportionality constant. As shown in Figure 5, the temperature dependence of the line widths is fitted properly by eq 2 with various E_a values (Table S3, Supporting Information). All of these results show the temperature effect expected for quadrupole relaxation; however, as can be seen in Figure 5 and Table S3, there are some differences in the E_a values, with that for Me-TACD being especially low.

^{13}C NMR Spectroscopy of Copper(I) Carbonyl Complexes. We also measured the ^{13}C NMR spectra of the copper bound ^{13}CO for several copper(I) carbonyl complexes, in order to examine the effect of the binding of CO to copper(I) ions from ^{13}C NMR spectroscopy. ^{13}C NMR signals of copper bound CO were observed only for ^{13}C-enriched carbonyl complexes because of the low natural abundance of ^{13}CO and broadening of the signal. As shown in Figure 6, the ^{13}C NMR signals of the copper bound ^{13}CO are observed around 175 ppm from TMS. The ^{13}C NMR signal of ^{13}CO gas in dichloromethane is observed at 184 ppm, thus, the ^{13}C NMR signals show an upfield shift with the binding of a copper(I) ion. This is in contrast to the ^{13}C NMR signals of heme-iron bound ^{13}CO, which were detected more downfield (∼200 ppm from TMS) compared to that of ^{13}CO gas.[56,57] Since the ^{13}C NMR shifts of the copper bound

(55) We found solvent effect on the ^{63}Cu NMR signal for (3,5-*i*Pr$_2$-TPB)-CuCO (Table S2, Supporting Information). The ^{63}Cu NMR chemical shift correlated with the acceptor number of the solvent. Similarly, the ν(C≡O) value for (3,5-*i*Pr$_2$-TPB)CuCO was also changed by the solvent. Interaction of a solvent with the copper bound CO would change the strength of the Cu−CO bond, resulting in the change in the ^{63}Cu NMR chemical shift and the ν(C≡O) value. On the other hand, the ^{63}Cu NMR line width did not correlate with the solvent viscosity but did correlate roughly with its ^{63}Cu NMR chemical shift. It seems that the effect on the solvent interaction to the copper complex is more significant to the ^{63}Cu NMR line width than that on the solvent viscosity.

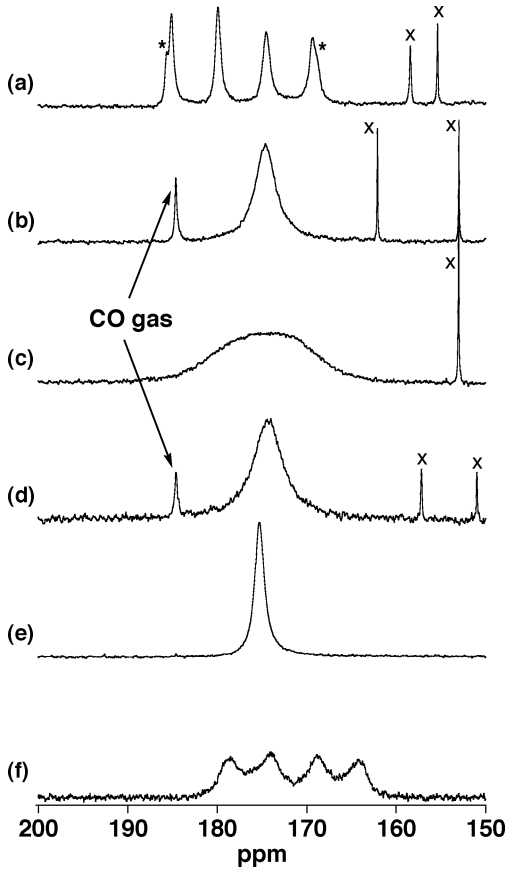

Figure 6. ^{13}C NMR spectra of the copper(I) carbonyl complexes, (a) (3,5-*i*Pr$_2$−TPB)Cu^{13}CO, (b) [(3,5-*i*Pr$_2$−TPM)Cu^{13}CO]ClO$_4$, (c) [(*i*Pr−TIC)Cu^{13}CO]ClO$_4$, (d) [(TPC)Cu^{13}CO]ClO$_4$, (e) [(Bn-TACN)Cu^{13}CO]ClO$_4$ in CD_2Cl_2, and (f) (Me-TACDCu^{13}CO)ClO$_4$ (6) in 1,2-$C_2D_4Cl_2$ at 298 K. Peaks shown by asterisks in spectrum (a) are the ^{13}C NMR signals of the copper bound ^{13}CO split by the hyperfine coupling with natural abundant ^{65}Cu nucleus (30.91%). Peaks shown by crosses are ^{13}C NMR signals resulting from the tridentate ligands.

^{13}CO of the copper(I) carbonyl complexes are observed in a narrow range (173.5−177.2 ppm), the electronic effect of the tridentate ligand does not affect the ^{13}C NMR shift (Figure S2, Supporting Information). Interestingly, the ^{13}C NMR signals of the copper bound ^{13}CO for (3,5-*i*Pr$_2$-TPB)-CuCO and (Me-TDCN)CuCO are separated into a quartet by the hyperfine coupling with ^{63}Cu (J = 663 and 586 Hz). Furthermore, as shown by asterisks in Figure 6a, the ^{13}C NMR signals resulting from the hyperfine coupling of the copper bound ^{13}CO with the naturally abundant ^{65}Cu nucleus (30.91%) are observed adjacent to the most downfield and upfield signals in the quartet signals of the copper bound ^{13}CO coupled with the ^{63}Cu nucleus. On the other hand, the ^{13}C NMR signals of the copper bound ^{13}CO for other copper-(I) carbonyl complexes are observed as a singlet. The hyperfine coupling of a ^{13}C NMR signal can be observed only for the complexes exhibiting extremely sharp ^{63}Cu NMR signals. For other copper carbonyl complexes exhibiting broad ^{63}Cu NMR signals, the Cu−^{13}C hyperfine coupling was not observed in their ^{13}C NMR signals because of the fast quadrupole relaxation processes of the copper(I) nuclei.

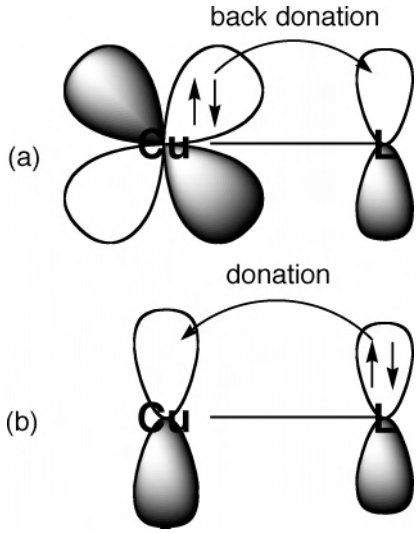

Figure 7. Illustration of the d and p mechanism of the ^{63}Cu NMR chemical shift. (a) d contribution, (b) p contribution. Although this figure is written for the p interactions, these mechanisms involve both σ and π interactions.

To further confirm a relationship of the Cu−^{13}C hyperfine coupling with the quadrupole relaxation process of copper, we examined temperature dependence of ^{13}C NMR signals of the copper bound CO (Figure S3, Supporting Information). With increasing temperature, the Cu−^{13}C hyperfine couplings of the ^{13}C NMR signals of the copper bound CO are more resolved. This is consistent to the idea that the loss of the Cu−^{13}C hyperfine coupling is due to rapid quadrupole relaxation of the copper nucleus, because the quadrupole relaxation rates of the copper nuclei for the copper(I) carbonyl complexes are slowed with increasing temperature, as shown in the previous section. On the other hand, as shown in the temperature dependence of ^{63}Cu NMR signal, a rapid exchange process of the copper bound CO is not so significant to the line shape of the^{13}C NMR signal of the copper bound CO because this process allows us to expect that the Cu−^{13}C hyperfine coupling is less resolved with increasing temperature.

Discussion

^{63}Cu NMR Spectroscopy. The copper(I) ion has a closed shell d^{10} electron configuration. Thus, the observed ^{63}Cu NMR chemical shifts for the copper(I) complexes examined here can be expressed by Ramsey's equation and divided into two terms; $\sigma = \sigma^D + \sigma^P$.[14−16] σ^D is a diamagnetic shielding term, which depends on the electron densities of the s orbitals in the ground state, and σ^P is a paramagnetic shielding term representing an energy gap between the ground and the excited states of p and/or d orbitals. Since the diamagnetic shielding term is primarily determined by the inner-shell molecular orbitals, it depends on the metal, its oxidation state, and its coordination number. On the other hand, the paramagnetic shielding term is caused by the donation of electrons from the ligands to the outer p orbitals of copper, a p contribution, and by the back-donation of electrons from the copper d orbitals to the ligands, a d contribution (Figure 7). A previous theoretical calculation by Nakatsuji et al.[24] showed that, for the ^{63}Cu NMR chemical

(56) Moon, R. B.; Richards, J. H. *Biochemistry* **1974**, *13*, 3437−3443.
(57) Moon, R. B.; Dill, K.; Richards, J. H. *Biochemistry* **1977**, *16*, 221−228.

shift of various copper(I) complexes, the paramagnetic contribution is a major factor and the diamagnetic contribution is almost constant and a minor factor. Furthermore, for the ^{63}Cu NMR shift, the d contribution is a major source of the paramagnetic shielding term, so the ^{63}Cu NMR chemical shift is determined by the electron acceptability of the ligand from a copper(I) ion. When a π-acceptor ligand is coordinated to a copper(I) ion, electrons are donated from the copper(I) ion to the ligand through the d_{π}(metal)-p_{π^*}(ligand) overlap, resulting in an electron density around copper(I) from the original d^{10} to d^{10-n}. The decrease in the electron density around copper(I) produces a downfield shift of the ^{63}Cu NMR signal. Therefore, the ^{63}Cu NMR signal for a copper(I) complex shifts downfield with increasing π acceptability of the ligand of the copper(I) ion. To the contrary, from the viewpoint of a copper ion, the ^{63}Cu NMR chemical shift is a measure of the electron density of the copper ion and indicates the extent to which the copper ion can donate electrons to ligands.

On the other hand, the ^{63}Cu NMR signal is only observable when the quadrupole relaxation is slow.[14−16] This is because the nuclear relaxation of ^{63}Cu with a nuclear spin $I = 3/2$ would be expected to be dominated by the quadrupole relaxation mechanism. The quadrupole relaxation rate is determined by the electronic field gradient around the nucleus. A uniform spherical orbital does not produce an electronic field gradient, leading to a slow quadrupole relaxation, but an ellipsoidal orbital forms an electronic field gradient around the nucleus resulting in a rapid quadrupole relaxation. As a result, the ^{63}Cu NMR signal is observable when the environment around the copper ion approaches a cubic symmetry and when the distorted environment around the copper ion causes the ^{63}Cu NMR signal to be unobservably broad. In fact, ^{63}Cu NMR signals were observed only for the copper complexes with a T_d symmetry, tetrahedral copper complexes binding with the same ligands.[17−32] For the quadrupole relaxation mechanism, the line width of the ^{63}Cu NMR signal indicates the symmetry of the electronic field around the copper nucleus. Other important factors affecting ^{63}Cu NMR line width are temperature and viscosity of a NMR sample and a ligand exchange process of a copper complex. The temperature and viscosity of the NMR sample change the correlation time (τ_Q), shown in eqs 1 and 2. With increasing the temperature or with decreasing the viscosity, a molecular rotation of a copper complex is faster and the correlation time is shorter. The viscosity of the sample is changed by the concentration or temperature of the sample. In general, the viscosity is decreased with increasing temperature or with decreasing the sample concentration. Consequently, at the same concentration, the ^{63}Cu NMR signal becomes sharper with increasing temperature, as shown in eq 2. On the other hand, the ^{63}Cu NMR line width is increased when the ligand exchange process of the copper complex is fast. The ligand-dissociated form, which lacks rigorous T_d symmetry, broadens the ^{63}Cu NMR signal because of the fast quadrupole relaxation rate. The ligand exchange process becomes faster with increasing temperature. Therefore, when the ligand exchange process is dominant for the ^{63}Cu NMR relaxation process, the ^{63}Cu NMR signal becomes boarder with increasing temepertaure.

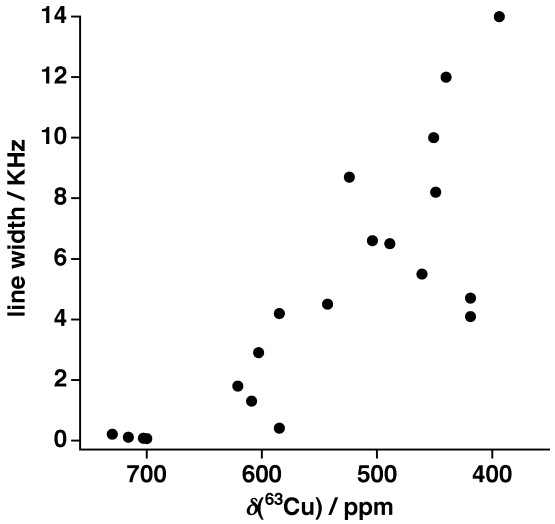

Figure 8. Relation between ^{63}Cu NMR chemical shifts and line widths ($W_{1/2}$) of the copper(I) carbonyl complexes. These data are summarized in Table 3.

^{63}Cu NMR Spectra of Copper(I) Complexes with Tridentate Ligands. The present ^{63}Cu NMR spectra of copper(I) complexes with various tridentate ligands can be interpreted on the basis of the above discussion. The copper(I) carbonyl complexes prepared in this study exhibit ^{63}Cu NMR signals in spite of the distorted tetrahedral geometries around copper(I) ions. As shown for [(*i*Pr-BITC)CuCO]ClO_4, the ^{63}Cu NMR signal of copper(I) carbonyl complexes is also detectable even with a much lower coordination symmetry around the copper ion. Furthermore, ^{63}Cu NMR signals of copper(I) carbonyl complexes with various tridentate ligands are sharper than the corresponding acetonitrile complexes. These results clearly indicate that the copper bound CO sharpens the ^{63}Cu NMR signal of a copper(I) complex. The participation of CO in line sharpening is further supported by the correlation between the ^{63}Cu NMR shift of the copper(I) carbonyl complex and its line width ($W_{1/2}$), as shown in Figure 8. Since the ^{63}Cu NMR shift of a copper(I) carbonyl complex is mainly determined by the Cu−CO bond, as discussed in detail below, the correlation suggests that bond characteristics of Cu−CO change the electronic field gradient around the copper ion. As suggested from the ^{63}Cu NMR chemical shift and the ν(C≡O) value, CO works as a good π-acceptor ligand to the copper(I) ion, but acetonitrile and triphenylphosphine do not. Therefore, the copper bound CO can accept an electron around the copper(I) ion in its antibonding orbital. The π acceptability of CO coincidentally cancels a donor effect of the tridentate ligand and changes an asymmetric charge distribution around the copper ion to one that is more symmetric. The symmetric electronic field gradient around the copper ion leads to a slow quadrupole relaxation, resulting in a sharp ^{63}Cu NMR signal.

Interestingly, copper(I) complexes having a phenyl substituent in their tridentate ligands exhibit broader ^{63}Cu NMR signals compared to the corresponding copper(I) complexes

with other substituents. The electronic effect of the phenyl group in a tridentate ligand, such as a ring current effect, may interact with the electronic field gradient around the copper ion. This would lower the symmetry of the charge distribution around the copper ion, resulting in a broad ^{63}Cu NMR signal for the phenyl substituent.

The temperature dependence of the ^{63}Cu NMR signals for the present copper(I) complexes with a tridentate ligand suggests that the quadrupole relaxation process, shown in eq 2, mainly determines the line widths of the ^{63}Cu NMR signals and suggests that the ligand exchange processes for these complexes are not so significant as to change the line widths. The slow ligand exchange for the present copper complexes may be due to a strong electron donor effect of the tridentate ligand, which strengthens the binding of the fourth ligand. Except for the Me-TACD complex, the activation energies, E_a, for re-orientation of copper complexes are reasonable compared to those expected from temperature dependence of solvent viscosity.[58] Thus, for these copper(I) complexes, solvent viscosity controls the correlation time, τ_Q, and ^{63}Cu NMR line width. On the other hand, for the Me-TACD complex, some intramolecular motion may contribute to τ_Q and to the narrowness of the ^{63}Cu NMR signal because the activation energy for the Me-TACD complex is much smaller than that for solvent viscosity. Large coordination space of Me-TACD may be related to the intramolecular motion. This is supported by the result that the Me-TACD complex is an outlier in Figure 8. Similarly, 3,5-Me$_2$-TPM and Me-TACN complexes are also outliers in Figure 8, maybe for the same reason as the Me-TACD complex. Overall, various line widths for the present copper complexes represent a symmetry of an electronic field gradient around the copper ion, which is modulated by electronic effects of the tridentate ligand and the fourth ligand, as discussed above.

The ^{63}Cu NMR signals of all copper(I) carbonyl complexes in this study show large downfield shifts, compared to the corresponding acetonitrile and triphenylphosphine complexes. Since CO is a good π-accepter ligand, the large downfield shift can be explained by the paramagnetic shielding effect caused by π back-donation from the copper d orbitals to the antibonding p* orbital of the copper bound CO, as discussed above. The paramagnetic shielding effect caused by CO expands the ^{63}Cu NMR shift range, similar to what is seen in NMR spectra of paramagnetic compounds. As a result, ^{63}Cu NMR signals of the copper(I) carbonyl complexes can be observed over a wide range depending on the tridentate ligand, although no drastic shifts are detected for the ^{63}Cu NMR spectra of copper(I) acetonitrile complexes. The difference in these ^{63}Cu NMR shifts of copper(I) carbonyl complexes is the result of the electron donor effect of the tridentate ligand. Overall, the copper bound CO amplifies small structural and electronic changes that occur around the copper ion to be easily detected in their ^{63}Cu NMR shifts.

(58) *CRC Handbook of Chemistry and Physics*, 86th ed.; Lide, D. R., Ed.; CRC Press: Boca Raton, FL, 2005.

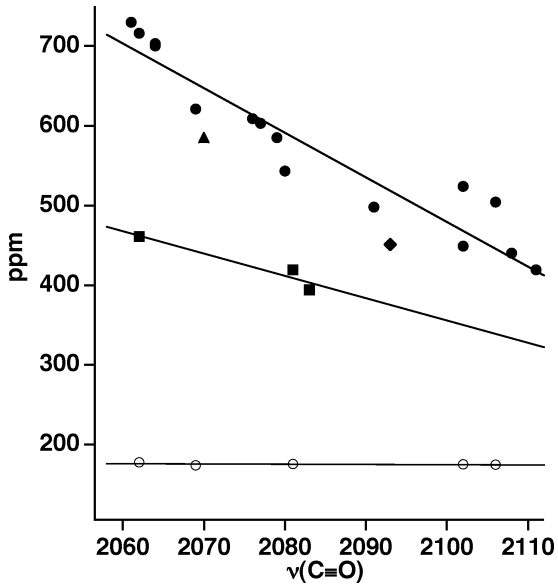

Figure 9. Correlation between NMR chemical shifts (^{63}Cu and ^{13}C) and C≡O stretching vibrations of copper(I) carbonyl complexes. Filled circles: ^{63}Cu NMR for the TPB, TPM, TIC, TPC, TPCME, and TPYM complexes. Filled squares: ^{63}Cu NMR for TACN complexes. Filled triangle: ^{63}Cu NMR for the TACD complex. Filled diamond: ^{63}Cu NMR for the BITC complex. Empty circles: ^{13}C NMR for (3,5-*i*Pr$_2$-TPB)Cu^{13}CO, [(3,5-*i*Pr$_2$-TPM)Cu^{13}CO]ClO$_4$, [(*i*Pr-TIC)Cu^{13}CO]ClO$_4$, [(TPC)Cu^{13}CO]ClO$_4$, and [(Bn-TACN)Cu^{13}CO]ClO$_4$. These data are summarized in Table 3.

Correlation of ^{63}Cu NMR Shift with C≡O Stretching Vibration. The utility of the copper bound CO is further supported by a linear correlation between the ^{63}Cu NMR shift of the copper(I) carbonyl complex and its ν(C≡O) value. In a previous paper,[30] we showed a linear correlation between the ^{63}Cu NMR shifts of copper(I) carbonyl complexes with the various hydrotris(1-pyrazolyl)borate (TPB) ligands and their ν(C≡O) values. As shown in Figure 9, the findings herein show that the ^{63}Cu NMR signals of all copper(I) carbonyl complexes other than those of TPB complexes are also correlated with their ν(C≡O) values and shift to a higher field with an increase in ν(C≡O) value. This correlation can be explained by the electronic donor effect of the tridentate ligand to the copper ion. With an increase in electron donation from the tridentate ligand, the electron density of the copper ion is increased, and the filled d orbitals of d^{10} copper(I) ion are destabilized by electronic repulsion. As a result, the π back-donation from copper(I) to the antibonding orbitals of the copper bound CO would be stronger. Therefore, the C≡O bond is weakened, and the ν(C≡O) value for the copper(I) carbonyl complex shifts to a lower wavenumber with an increase in the donor effect of the tridentate ligand. Similarly, with an increase in the donor effect, the ^{63}Cu NMR shift of the copper(I) carbonyl complex is shifted downfield because the large paramagnetic shielding effect is induced by the strong π back-donation. Consequently, the ^{63}Cu NMR shift of the copper(I) carbonyl complex correlates with its ν(C≡O) value. This correlation indicates that the ^{63}Cu chemical shift of the copper(I) carbonyl complex is a sensitive measure of the electron donor ability of the ligand of a copper(I) complex.

Interestingly, the correlation line for the copper carbonyl complex with the imino-type, sp^2 N ligand is different from

that for the amino-type, sp^3 N ligand. This is due to the difference in the characteristics of the ligand N−Cu bond between the imino-type ligand and the amino-type ligand. The imino-type ligand binds to a copper ion via the σ and π orbitals of the imino nitrogen atom in the ligand while the amino-type ligand binds with the σ orbital of the amino nitrogen atom. The imino-type ligand can accept electrons by π back-donation from a copper ion in a π^* orbital, but the amino-type ligand cannot. This is supported by the Cu−N (ligand) bond lengths. As shown in the X-ray crystal structures of copper(I) carbonyl complexes (Figure 2 and Table 2), the Cu−N (ligand) bond lengths of the imino-type ligands are shorter than those of the amino-type ligands. Therefore, an additional paramagnetic shielding effect would be induced at the copper ion for the imino-type ligand, resulting in a downfield shift of the correlation line. This would also explain the deviation for [(*i*Pr-BITC)CuCO]ClO_4 from the correlation lines for the imino-type ligand. The decrease in the π acceptability of [(*i*Pr-BITC)CuCO]ClO_4 by replacing one imidazole ring with an sp^3-type thioether donor may result in smaller downfield shift of the ^{63}Cu NMR signal than the expected shift from the correlation line (Figure 9). On the other hand, we also found that [(Me-TACD)-CuCO]ClO_4 deviates from the correlation line for the amino-type ligand. Although we were not able to obtain the crystal structure of [(Me-TACD)CuCO]ClO_4, the crystal structure of [(*i*Pr-TACD)Cu]ClO_4[50] showed a drastic change in coordination structure from other copper complexes with tridentate ligands. Because of the large 12-membered macrocycle, the copper ion resides deep within the macrocycle with a Cu−N (ligand) bond distance (2.019−2.026 Å) shorter than those (2.09−2.15 Å) observed for other amino-type copper complexes. Furthermore, the coordination structure of *i*Pr-TACD to copper ion adopts a unique pyramidal geometry; N−Cu−N angles: 113−117°. These significant structural changes observed for the *i*Pr-TACD complex would be applicable to the Me-TACD complex and increase the electron density of the copper(I) ion, leading to a downfield deviation from the correlation line.

The strong correlation between the ^{63}Cu NMR shift of a copper(I) carbonyl complex and its ν(C≡O) value implies that the ^{13}C NMR shift of the copper bound ^{13}CO of a copper-(I) carbonyl complex is also correlated with its ν(C≡O) value. However, as shown in Figure 9 and Figure S2, the ^{13}C NMR shift of the copper bound CO is not correlated with its ν(C≡O) value. Therefore, the ^{13}C NMR shift of the copper bound CO is not a good measure of the electronic donor ability of the ligand. In contrast to the ^{63}Cu NMR shift, both paramagnetic and diamagnetic shielding effects for the ^{13}CO are changed by the binding of the copper(I) ion. Since the change in the diamagnetic shielding effect is comparable to the change in the paramagnetic shielding effect on the ^{13}C NMR shift and these effects can cancel each other, the observed ^{13}C NMR shifts of the copper bound ^{13}CO are nearly constant for all complexes. As a result, the ^{13}C NMR shift of the copper bound CO of the copper carbonyl complex does not correlate with its ν(C≡O) value, in a straightforward manner.

In summary, we report a ^{63}Cu NMR spectroscopy for copper(I) complexes with various tridentate ligands. Copper-(I) carbonyl complexes with various tridentate ligands give ^{63}Cu NMR signals in spite of their C_3 symmetry around copper(I) ions. Furthermore, the paramagnetic shielding effect caused by the copper bound CO induces a large downfield shift of the ^{63}Cu NMR signal for the copper(I) carbonyl complex, which amplifies small structural and electronic changes caused by the ligand, making them easily detected. The findings herein indicate that CO complexation makes ^{63}Cu NMR spectroscopy much more useful for Cu(I) chemistry.

Appendix

Abbreviations. TPB, hydrotris(1-pyrazolyl)borate; 3,5-Me_2-TPB, hydrotris(3,5-dimethyl-1-pyrazolyl)borate; 3,5-*i*Pr_2-TPB, hydrotris(3,5-diisopropyl-1-pyrazolyl)borate; 3-*t*Bu-5-Me-TPB, hydrotris(3-tertiarybutyl-5-methyl-1-pyrazolyl)borate; 3-*t*Bu-5-*i*Pr-TPB, hydrotris(3-tertiarybutyl-5-isopropyl-1-pyrazolyl)borate; 3-*Ph*-5-*i*Pr-TPB, hydrotris(3-phenyl-5-isopropyl-1-pyrazolyl)borate; 3,5-Ph_2-TPB, hydrotris(3,5-diphenyl-1-pyrazolyl)borate; TPM, tris(1-pyrazolyl)methane; 3,5-Me_2-TPM, tris(3,5-dimethyl-1-pyrazolyl)methane; 3,5-*i*Pr_2-TPM, tris(3,5-diisopropyl-1-pyrazolyl)methane; 3,5-Ph_2-TPM, tris(3,5-diphenyl-1-pyrazolyl)methane; TIC, tris(1-methyl-4-imidazolyl)carbinol; Et-TIC, tris(1-methyl-2-ethyl-4-imidazolyl)carbinol; *i*Pr-TIC, tris(1-methyl-2-isopropyl-4-imidazolyl)carbinol; Ph-TIC, tris(1-methyl-2-phenyl-4-imidazolyl)carbinol; TPC, tris(2-pyridyl)carbinol; TPME, tris(2-pyridyl)methyl methyl ether; TPYM, tris(2-pyridyl)-methane; TACN, 1,4,7-triazacyclononane; Me-TACN, 1,4,7-trimethyl-1,4,7-triazacyclononane; Bn-TACN, 1,4,7-tribenzyl-1,4,7-triazacyclononane; *i*Pr-TACN, 1,4,7-triisopropyl-1,4,7-triazacyclononane; TACD, 1,5,9-triazacyclododecane; Me-TACD, 1,5,9,-trimethyl-1,5,9-triazacyclododecane; *i*Pr-TACD, 1,5,9,-triisopropyl-1,5,9-triazacyclododecane; iPr-BITC, bis(1-methyl-2-isopropyl-4-imidazaolyl)phenylthiomethylcarbinol.

Acknowledgment. This work was supported by grants from the Ministry of Education, Culture, Sports, Science and Technology, Japan, and from the Japan Science and Technology Agency, CREST.

Supporting Information Available: IR spectra of [(*i*Pr-TACN)CuCO]ClO_4 in the solid state (KBr) and in dichloromethane solution (Figure S1), plots of ^{13}C NMR shifts of copper(I) carbonyl complexes over their ν(C≡O) value (Figure S2), temperature dependence of ^{63}Cu and ^{13}C NMR signals for copper(I) complexes (Figures S3 and S4), ^{63}Cu and ^{13}C NMR and ν(C≡O) data for copper(I) complexes (Tables S1 and S2), activation energies for copper(I) complexes (Table S3), X-ray crystallographic files in CIF format for [(*i*Pr−TIC)CuCO]ClO_4, [(Me-TACN)CuCO]ClO_4, and [(Bn-TACN)CuCO]ClO_4. This material is available free of charge via the Internet at http://pubs.acs.org.

IC060745R